Photochemical & Photobiological Sciences (2021) 20:653–661
https://doi.org/10.1007/s43630-021-00051-9

ORIGINAL PAPERS

Low-power infrared laser modulates telomere length in heart tissue from an experimental model of acute lung injury

Larissa Alexsandra da Silva Neto Trajano[1,2,3] · Luiz Philippe da Silva Sergio[2] · Diego Sá Leal de Oliveira[2] · Eduardo Tavares Lima Trajano[3] · Marco Aurélio dos Santos Silva[3] · Flavia de Paoli[4] · André Luiz Mencalha[2] · Adenilson de Souza da Fonseca[2,5]

Received: 11 November 2020 / Accepted: 28 April 2021 / Published online: 19 May 2021

Abstract

Acute lung injury and acute respiratory distress syndrome can occur as a result of sepsis. Cardiac dysfunction is a serious component of multi-organ failure caused by severe sepsis. Telomere shortening is related to several heart diseases. Telomeres are associated with the shelterin protein complex, which contributes to the maintenance of telomere length. Low-power infrared lasers modulate mRNA levels of shelterin complex genes. This study aimed to evaluate effects of a low-power infrared laser on mRNA relative levels of genes involved in telomere stabilization and telomere length in heart tissue of an experimental model of acute lung injury caused by sepsis. Animals were divided into six groups, treated with intraperitoneal saline solution, saline solution and exposed to a low-power infrared laser at 10 J cm^{-2} and 20 J cm^{-2}, lipopolysaccharide (LPS), and LPS and, after 4 h, exposed to a low-power infrared laser at 10 J cm^{-2} and 20 J cm^{-2}. The laser exposure was performed only once. Analysis of mRNA relative levels and telomere length by RT-qPCR was performed. Telomere shortening and reduction in mRNA relative levels of TRF1 mRNA in heart tissues of LPS-induced ALI animals were observed. In addition, laser exposure increased the telomere length at 10 J cm^{-2} and modulated the TRF1 mRNA relative levels of at 20 J cm^{-2} in healthy animals. Although the telomeres were shortened and mRNA levels of TRF1 gene were increased in nontreated controls, the low-power infrared laser irradiation increased the telomere length at 10 J cm^{-2} in cardiac tissue of animals affected by LPS-induced acute lung injury, which suggests that telomere maintenance is a part of the photobiomodulation effect induced by infrared radiation.

Keywords Low-power laser · Telomerase · Telomere length

✉ Larissa Alexsandra da Silva Neto Trajano
larissa.alexsandra@hotmail.com

[1] Mestrado Profissional em Diagnóstico em Medicina Veterinária, Universidade de Vassouras. Avenida Expedicionário Oswaldo de Almeida Ramos, 280, Vassouras, , Rio de Janeiro 27700000, Brazil

[2] Departamento de Biofísica e Biometria, Instituto de Biologia Roberto Alcântara Gomes, Universidade do Estado do Rio de Janeiro, Avenida 28 de Setembro, 87, fundos, Vila Isabel, Rio de Janeiro 20551030, Brazil

[3] Mestrado Profissional em Ciências Aplicadas em Saúde, Universidade de Vassouras, Avenida Expedicionário Oswaldo de Almeida Ramos, 280, Vassouras, Rio de Janeiro 27700000, Brazil

[4] Departamento de Morfologia, Instituto de Ciências Biológicas, Universidade Federal de Juiz de Fora, Minas Gerais, Rua José Lourenço Khelmer – s/n, Campus Universitário, São Pedro, Juiz de Fora 36036900, Brazil

[5] Centro de Ciências da Saúde, Centro Universitário Serra Dos Órgãos, Avenida Alberto Torres, 111, Teresópolis, Rio de Janeiro 25964004, Brazil

1 Introduction

Acute respiratory distress syndrome (ARDS) is a complex process and most serious form of Injury (ALI) [1], with approximately 150,000 individuals diagnosed with ARDS in the United States and approximately 1 million people worldwide annually. ARDS has different etiologies and can result in respiratory failure and death [1, 2]. Currently, the Severe Acute Respiratory Syndrome Coronavirus 2 (SARS-CoV-2) pandemic has increased the interest in understanding the ARDS [3]. Patients infected with coronavirus disease 19 (COVID-19) have flu-like symptoms, rapidly evolving into ARDS [4, 5]. ARDS may result from a direct lung injury, pneumonia, aspiration of gastric contents, inhalational injury or indirect lung injury, severe trauma, acute pancreatitis, and sepsis [6].

Sepsis often progresses to ALI, ARDS, and bilateral pulmonary infiltration [7], affecting more than 19 million people annually. Although the hospital mortality has decreased, from 35% in 2000 to 18% in 2012, patients who survive sepsis often experience new symptoms, prolonged disability, and worsening of health conditions [8]. Multi-organ failure represents the most severe consequence of sepsis and septic shock, associated with high mortality rates and long-term morbidity in survivors [9]. Cardiac dysfunction is a serious component of multi-organ failure, caused by a severe sepsis [10] and characterized by an impaired contractility, diastolic dysfunction, reduced cardiac index, and ejection fraction [11]. Approximately 50% of the patients diagnosed with sepsis exhibit signs of myocardial dysfunction [12].

Interestingly, increased risk of myocardial dysfunction, ischemic heart disease, early death, and heart failure has been associated with telomere shortening [13–16]. Also, telomere length analyses in biopsied diseased heart tissues and cardiomyocytes demonstrated the association between telomere shortening in adult heart affected by cardiac diseases and heart failure [15–17].

In 2009, telomeres were recognized as a fundamental aspect of cell biology with the Nobel Prize in Physiology or Medicine awarded to researchers who discovered how chromosomes are protected by telomeres and telomerases [18]. Telomeres are repetitive nucleoprotein structures at the chromosome ends [19]. Telomere shortening occurs with a decrease in the number of these repetitions and is associated with cell senescence and apoptosis [20]. The maintenance of the telomere length is influenced by a protein complex, the Shelterin proteins, which allows cells to distinguish the natural ends of chromosomes from sites of DNA damage [21, 22]. Shelterin is a six-subunit protein complex including telomere repeat binding factors 1 and 2 (TRF1 and TRF2), TRF1-interacting protein 2 (TIN2), protection of telomere protein 1 (POT1), TIN2 and POT1 interacting protein (TPP1), and repressor/activator protein 1 (RAP1) [20].

Previous studies have demonstrated modulation of mRNA levels from shelterin complex genes after exposure to a low-power infrared laser [23, 24]. These lasers are considered safe and effective nonionizing sources with well-established photobiomodulation effect on cells and tissues in the so-called therapeutic window [25, 26, 26]. In a study, it was demonstrated that exposure to a low-power infrared laser increases the mRNA levels of TRF1 and TRF2 genes in myoblasts, which can conibute to telomere stabilization [23]. In another study, mRNA relative levels of TRF1 and TRF2 genes were modulated by a low-power infrared laser in injured skeletal muscle in an experimental model of muscle injury [24].

Although the effects of low-power infrared lasers on the telomere stability in cells and tissue have been evaluated [23, 24], no studies have been carried out to evaluate the photobiostimulation effect of a low-power infrared laser on the telomere stabilization in healthy or diseased heart tissue. Thus, this study aimed to evaluate effect of a low-power infrared laser on mRNA relative levels of genes involved in telomere stabilization and telomere length in heart tissue from an experimental model of acute lung injury by sepsis.

2 Materials and methods

2.1 Low-power laser

A therapeutic low-power infrared (808 nm) laser (Photon Lase III, AsGaAl), purchased from D.M.C. Equipamentos Ltda (São Paulo, Brazil), in the continuous-wave emission mode was used in this study. The laser parameters are presented in Table 1.

Table 1 Photobiomodulation physical parameters

Wavelength	808 nm
Power	100 mW
Spot size	0.028 cm^2
Power density	3.541 W cm^{-2}
Energy per point	0.28 J and 0.56 J
Energy density	10 J cm^{-2} and 20 J cm^{-2}
Time per point	2 s and 5 s
Number of points in heart	1
Application technique	Punctual by skin contact

2.2 Experimental procedure

Thirty male Wistar rats (mass: 285.0 ± 22.9 g) were obtained from the Departamento de Ciências Fisiológicas vivarium (Universidade Federal do Estado do Rio de Janeiro, Brazil). All animals were 3–4 months old at the time of the experiment. The animals were kept in an animal room with controlled environmental conditions (12 h light/12 h dark, 22 °C) on closed ventilated shelves. The animals received rat chow pellets and water ad libitum. The ALI by sepsis was induced by intraperitoneal administration of lipopolysaccharide (LPS) from *Escherichia coli* (Sigma-Aldrich, USA) at 10 mg kg^{-1}. LPS-induced animal model causes acute injury to the epithelial and endothelial barriers in the lungs [27]. LPS activates alveolar macrophages, through which neutrophils infiltrate and damage the lungs. Neutrophils produce additional cytokines, which have a crucial role as signaling molecules that initiate and perpetuate inflammatory response at the local and systemic levels [28], which has been used in an experimental model, similar to ALI/ARDS in humans [27].

For the experimental procedure, animals were anesthetized with an intraperitoneal bolus of ketamine (80 mg kg^{-1}) and xylazine (8 mg kg^{-1}) [29], and then randomly assigned to six main groups of five animals each: (1) CONTROL GROUP were animals treated with an intraperitoneal saline solution (0.9% NaCl); (2) LASER-10 were animals treated with an intraperitoneal saline solution and, after 4 h, exposed to an infrared laser at 10 J cm^{-2}; (3) LASER-20 were animals treated with an intraperitoneal saline solution and, after 4 h, exposed to an infrared laser at 20 J cm^{-2}; (4) ALI (acute lung injury) were animals treated with an intraperitoneal LPS (10 mg kg^{-1}); (5) ALI-LASER10 were animals treated with an intraperitoneal LPS (10 mg kg^{-1}) and, after 4 h, exposed to an infrared laser at 10 J cm^{-2}; (6) ALI-LASER20 were animals treated with an intraperitoneal LPS (10 mg kg^{-1}) and, after 4 h, exposed to an infrared laser at 20 J cm^{-2}. All groups were manipulated simultaneously. LPS solutions were prepared in a saline solution immediately before use to induce ALI. The protocol for the induction of ALI by LPS has been reported [26, 28, 30, 31]. ALI was observed after 24 h.

Laser irradiation was performed after sedation with an intraperitoneal bolus of ketamine (80 mg kg^{-1}) and xylazine (8 mg kg^{-1}), at the dorsal decubitus position, and trichotomy of the thoracic region of the animals. The irradiation was performed only once at a single point above the heart. The low-power infrared laser exposure was carried out 4 h after the ALI induction. 24 h after the LPS-induced ALI or after the irradiation procedure, the animals were euthanized with anesthetic over-dose and laparotomy was performed for heart removal and further analysis. This study was approved by the Universidade Federal de Juiz de Fora Research Ethics Committee, Minas Gerais, Brazil (process number 012/2016).

2.3 DNA extraction

After the euthanasia, samples of heart tissue were collected and transferred to microcentrifuge flex tubes with TRIzol® reagent for total RNA extraction using a standard procedure. TRIzol® reagent was added and samples were crushed in microcentrifuge flex tubes and centrifuged (12,000 *g*, 4 °C, 5 min). Supernatants were transferred to other tubes, chloroform was added, mixtures were centrifuged (12,000 *g*, 4 °C, 15 min), aqueous phases were transferred to other tubes, and isopropanol was added. After incubation (room temperature, 15 min), the mixtures were centrifuged (12,000 *g*, 4 °C, 10 min), supernatants were discarded, and the precipitate was washed with an ethanol–DEPC (80% ethanol, 0.1% DEPC) solution and centrifuged. DNA was suspended in NaOH and the mixtures were centrifuged (12,000 *g*, 4 °C, 10 min). The supernatant was transferred to other tubes, the pH was adjusted, and the samples were stored (-20 °C). The experimental protocol for DNA extraction was performed according to the manufacturer's instructions (TRIzol® reagent, Invitrogen, USA).

2.4 Telomere measurement

The telomere length was measured by real time PCR as proposed by Cawthon [32]. The telomere primers were tel 1 at 270 nM and tel 2 at 900 nM. The reference gene was 36B4. The sequences of the genes analyzed by RT-qPCR are listed in Table 2. The final 36B4 (single-copy gene) primer concentrations were: 36B4u and 36B4u at 300 nM. For telomere RT-qPCR, 18 cycles at 95 °C for 15 s and at 54 °C for 2 min were carried out. For 36B4 PCR, 30 cycles at 95 °C for 15 s and at 58 °C for 1 min were carried out. The reactions were run on an Applied Biosystems 7500 RT-qPCR machine (Applied Biosystems, USA). Duplicate CT values were analyzed in Microsoft Excel (Microsoft) using the comparative

Table 2 Sequences of the analyzed genes by RT-qPCR

Tel	Forward (tel 1): 5′-GGTTTTTGAGGGTGAGGG TGAGGGTGAGGGTGAGGGT -3′ Reverse (tel 2): 5′- TCCCGACTATCCCTATCC CTATCCCTATCCCTATCCCTA -3′
36D4	Forward: 5′- ACTGGTCTGGGGCCTGAGAAG -3′ Reverse: 5′- TCAATGATACCTCTGGAGATT -3
TRF1	Forward: 5′- AGTTGCAGCAGGAAAGTCTCT -3′ Reverse: 5′- GGGCTGATTCCAAGGGTGTA -3′
TRF2	Forward: 5′- GCAGAAGATGTTGCGCTTCC -3′ Reverse: 5′- CCACTGGCTCTGTGTGCTTT -3′
GAPDH	Forward: 5′- ATGATTCTACCCACGGCAAG -3′ Reverse: 5′- CTGGAAGATGGTGATGGGTT -3′

CT (2 – ΔΔCT) method [33]. RT-qPCR for each sample was performed in duplicate.

2.5 Total RNA extraction

After the euthanasia, samples of heart tissue were collected and transferred to microcentrifuge flex tubes with TRIzol® reagent for total RNA extraction using a standard procedure. TRIzol® reagent was added and samples were crushed in microcentrifuge flex tubes and centrifuged (12,000 *g*, 4 °C, 5 min). Supernatants were transferred to other tubes, chloroform was added, mixtures were centrifuged (12,000 *g*, 4 °C, 15 min), aqueous phases were transferred to other tubes, and isopropanol was added. After incubation (room temperature, 15 min), the mixtures were centrifuged (12,000 *g*, 4 °C, 10 min), supernatants were discarded, and precipitates were washed with an ethanol–DEPC (80% ethanol, 0.1% DEPC) solution and centrifuged. Supernatants were withdrawn and total RNA was reconstituted in a water–DEPC (0.1%) solution and stored (– 80 °C). The experimental protocol for DNA extraction was performed according to the manufacturer's instructions (TRIzol® reagent, Invitrogen, USA).

2.6 Complementary DNA synthesis

The RNA concentration and purity were determined using a spectrophotometer by calculating the optical density ratio at a wavelength ratio of 260 nm/280 nm. The Complementary DNA (cDNA) synthesis was carried out using a two-step cDNA synthesis kit (Promega, USA). Four micrograms of RNA were reverse-transcribed into cDNA using GoScript™ reverse transcriptase (Promega, USA), according to the manufacturer's protocol, using a 20 µL total reaction. RT-qPCR was performed using 5 µL of GoTaq qPCR Master Mix (Promega) for a final volume of 10 µL containing 50 ng of cDNA. To determine the initial relative quantity of cDNA, samples were amplified with Telomere repeat binding factor 1 (TRF1), Telomere repeat binding factor 2 (TRF2), and glyceraldehyde-3-phosphate dehydrogenase (GAPDH) primers. The sequences of the genes analyzed by RT-qPCR are listed in Table 2. The reactions were run on an Applied Biosystems 7500 RT-qPCR machine (Applied Biosystems, USA). The mixtures were initially denatured at 95 °C for 10 min. For TRF1 and TRF2 RT-qPCR, 40 cycles at 95 °C for 20 s and at 60 °C for 45 s were carried out. Melt curve analyses were performed for all genes. The specificity and integrity of the PCR products were confirmed by the presence of a single peak. The relative expression was normalized to that of the reference gene (GAPDH). Duplicate CT values were analyzed in Microsoft Excel (Microsoft) using the comparative CT (2 – ΔΔCT) method [33]. RT-qPCR for each sample was performed in duplicate.

2.7 Statistical analysis

Data are reported as the mean ± standard deviation. The Mann–Whitney test was performed to compare the data of the ALI group to those of the control group. The comparison was performed using data normalization with the control group. The One-way Analysis of Variance (ANOVA) test was performed to verify possible statistical differences, followed by the Tukey's post hoc test. The Kolmogorov–Smirnov test was performed to verify the normality distribution of the data. Data from relative mRNA levels were normalized to the control group to compare the animals exposed to a low-power infrared laser to the animals of the control group. Data from relative mRNA levels were normalized to the ALI group to compare the animals affected by ALI to those affected by ALI and exposed to the low-power infrared laser. The level of significance was set at $p < 0.05$. The InStat Graphpad software was used to perform a statistical analysis (GraphPad InStat version 5.0 for Windows 8, GraphPad Prism Software, San Diego, CA, USA).

3 Results

3.1 Telomere length in heart tissue of the normal and LPS-induced ALI groups

Figure 1 shows the relative telomere length in the heart tissue of animals after the LPS-induced ALI. Data in this figure show a significant ($p < 0.05$) decrease in relative telomere length in the heart tissue from the animals of the ALI group when normalized and compared to the control group.

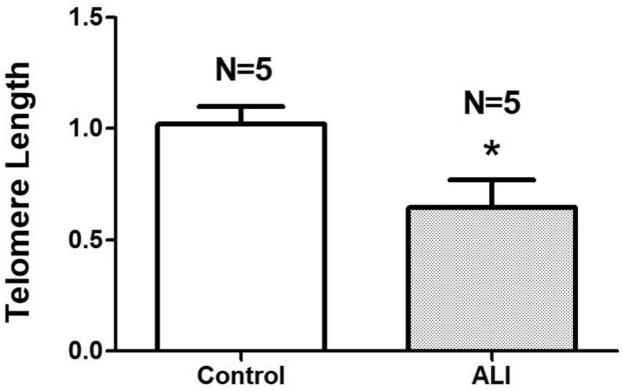

Fig. 1 Relative telomere length of normal and LPS-induced ALI animals. Wistar rats were inoculated with LPS, samples of heart tissue were collected, genomic DNA was extracted, and real time quantitative polymerase chain reactions were performed. (*) $p < 0.05$, compared to the control group. LPS: lipopolysaccharide. ALI: acute lung injury. $n = 5$: number of animals per group

3.2 Relative TRF1 and TRF2 mRNA levels in heart tissue of the normal and LPS-induced ALI groups

Figure 2 shows the relative mRNA levels of TRF1 and TRF2 genes in the heart tissue of animals after the LPS-induced ALI. These data show a significant ($p < 0.001$) decrease in relative TRF1 mRNA levels in the heart tissue of the ALI group when normalized and compared to the control group (Fig. 2a). Data in Fig. 2b do not show significant ($p > 0.05$) changes in the relative mRNA levels of TRF2 gene in the heart tissue of rats after LPS-induced ALI, normalized and compared to the control group.

3.3 Effects of the low-power infrared laser on the telomere length

Figure 3 shows the relative telomere length in heart tissue of the normal and LPS-induced ALI animals after the low-power infrared laser irradiation. The data in Fig. 3a show a significant decrease ($p < 0.01$) in the telomere length in the heart tissue of healthy animals exposed to the laser at 10 J cm^{-2}. Figure 3b shows a significant increase ($p < 0.01$) in the telomere length in the heart tissue of the LPS-induced ALI animals exposed to the laser at 10 J cm^{-2}.

3.4 Effects of the low-power infrared laser on the TRF1 and TRF2 mRNA levels

Figure 4 shows the relative mRNA levels of the TRF1 and TRF2 genes in the heart tissue of the normal and LPS-induced ALI animals after the low-power infrared laser irradiation. Data in Fig. 4a show a significant increase ($p < 0.05$) in the relative mRNA levels of TRF1 gene in heart tissue of healthy animals exposed to the laser at 20 J cm^{-2}. Notably, no significant changes ($p > 0.05$) in the relative mRNA levels of TRF1 gene in the heart tissue of the LPS-induced ALI animals exposed to the laser at 10 and 20 J cm^{-2} were observed. Data in Fig. 4b do not show significant ($p > 0.05$) changes in the relative mRNA levels of TRF2 gene in the heart tissue of the normal (control group) and LPS-induced ALI animals exposed to the laser at 10 and 20 J cm^{-2}.

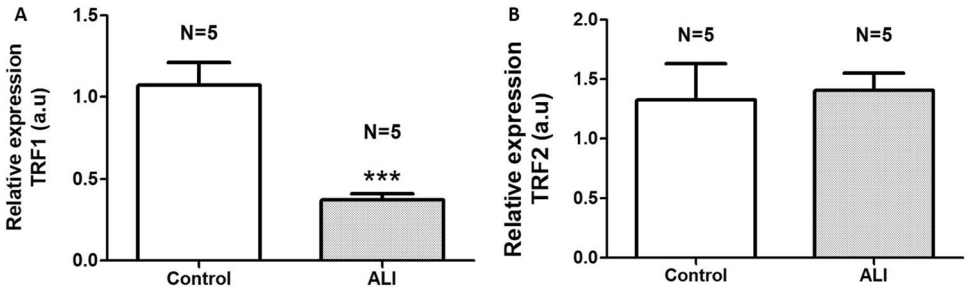

Fig. 2 Relative mRNA levels of TRF1 (**a**) and TRF2 (**b**) genes of normal and LPS-induced ALI animals. Wistar rats were inoculated with LPS and heart tissue samples were collected, total RNA extraction, complementary DNA synthesis and real time quantitative polymerase chain reactions were performed. (***) $p < 0.001$, compared to the control group. LPS: lipopolysaccharide. ALI: Acute Lung Injury. $n = 5$: number of animals per group

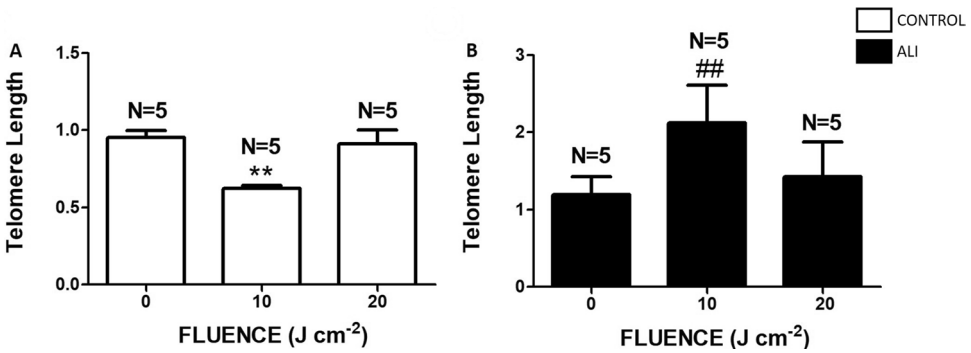

Fig. 3 Relative telomere length of normal (**a**) and LPS-induced ALI (**b**) animals. Wistar rats were inoculated with LPS and, after 4 h, exposed to the low-power infrared laser at different fluences. Samples of heart tissue were collected, genomic DNA was extracted, and real time quantitative polymerase chain reactions were performed. (**) $p < 0.05$, compared to the control group, not irradiated; (##) $p < 0.05$, compared to the ALI group not irradiated. LPS: lipopolysaccharide. ALI: Acute Lung Injury. n = 5: number of animals per group

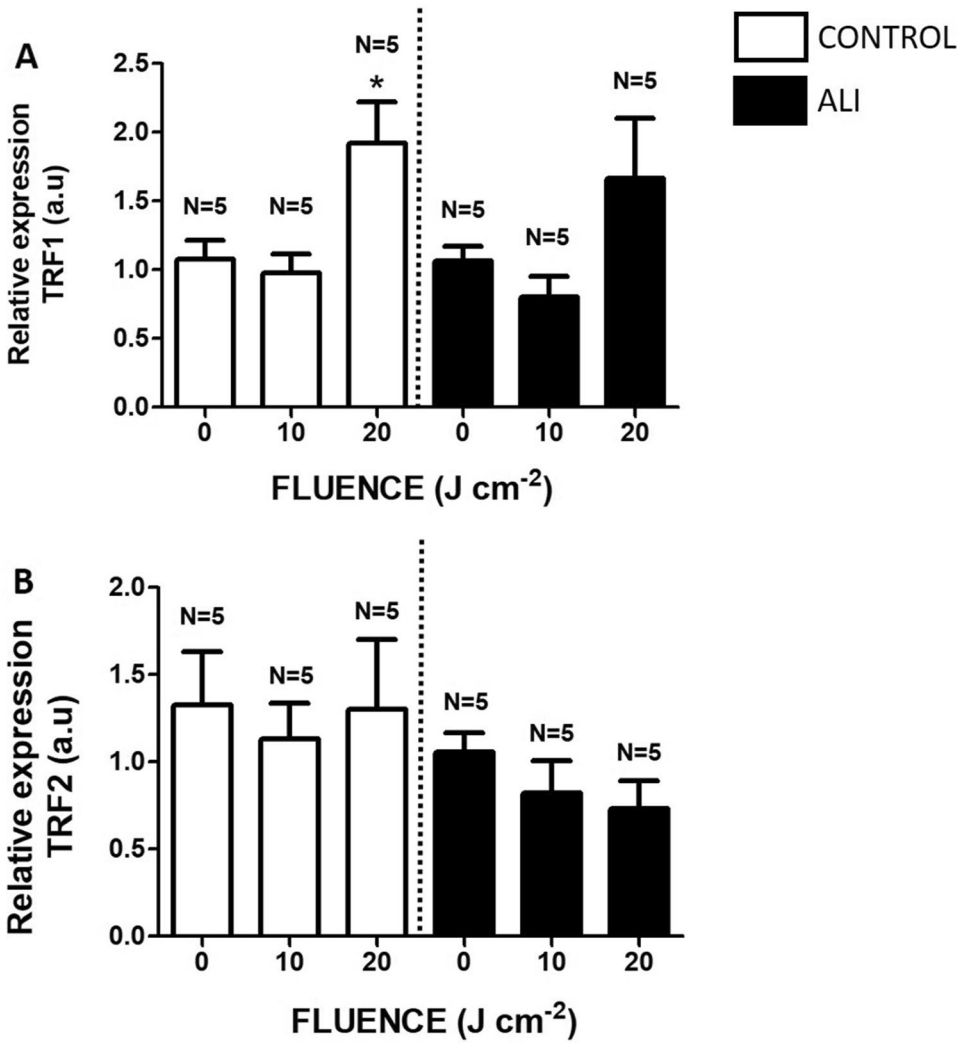

Fig. 4 Relative mRNA levels of TRF1 (**a**) and TRF2 (**b**) genes of normal and LPS-induced ALI animals. Wistar rats were inoculated with LPS and, after 4 h, exposed to the low-power infrared laser at different fluences. Heart tissue samples were collected, total RNA extraction, complementary DNA synthesis, and real time quantitative polymerase chain reaction were performed. (*) $p < 0.05$, compared to the control group not irradiated. LPS: lipopolysaccharide. ALI: Acute Lung Injury. n = 5: number of animals per group

4 Discussion

Our results show telomere shortening in heart tissue of rats after the LPS-induced ALI, which suggests that the telomere shortening of chromosomes in the hearts of animals was affected by sepsis (Fig. 1). A reduction in the relative mRNA levels of TRF1 gene was also observed in the cardiac tissue of these animals. However, no significant difference in the relative mRNA levels of TRF2 gene was observed in rats with LPS-induced ALI (Fig. 2). TRF1 and TRF2 are important proteins for the maintenance of the telomere length [34, 35]. These results suggest that the reduction in mRNA relative levels of TRF1 gene is related to telomere shortening in rats affected by LPS-induced ALI. Although telomere shortening has been proposed as a general risk factor for age-related chronic diseases, such as cancer, type-2 diabetes, and cardiovascular disease [36], few studies evaluated the telomere length in heart tissue [13–16], while no studies evaluated the telomere length and mRNA relative levels from genes from telomere stabilization in heart tissue in experimental models of ALI by sepsis. The mechanisms involved in sepsis have yet to be elucidated [37]. However, some authors suggested that telomere dysfunction can contribute to critical illness outcomes [37, 38]. Other authors suggested that telomere shortening is associated with a higher risk of ischemic heart disease [39], increased risk of coronary heart disease [39], and heart failure. Hypertrophic hearts with a reduced ejection fraction exhibit the shortest telomeres [16]. In addition, an autopsy of myocardial tissue showed that heart disease has been associated with telomere shortening [15].

The data in Fig. 3a suggest that irradiation with a low-power infrared laser at 10 J cm^{-2} caused telomere shortening in healthy tissue. Studies have already shown that the low-power laser could modify the expression of genes related to the nucleotide excision repair pathway, even in the skin and skeletal muscle of healthy Wistar rats, suggesting laser-induced modulation of DNA repair and genomic stability [25, 40]. Such studies corroborate our results, suggesting that, depending on the laser parameters,

the low-power laser irradiation can modulate the telomere length in healthy animals. Notably, no telomere shortening was observed in healthy animals irradiated with a laser at 20 J cm^{-2}. A study on the evaluation of the influence of a low-power laser therapy on parameters of oxidative stress and DNA damage in skeletal muscle and plasma of rats with heart failure demonstrated that the DNA damage index had a significant increase at 21 J cm^{-2} compared to that at 3 J cm^{-2}, which suggests that high doses of a low-power laser seem to increase the DNA damage [41]. On the other hand, a study on the evaluation of DNA damage in blood cells of healthy animals after red and infrared laser irradiations demonstrated that the DNA damage is not dependent on the fluence because the irradiation at 50 J cm^{-2} induced higher levels of DNA damage in blood cells than those at 25 and 100 J cm^{-2} [42]. Although these data suggest DNA damage after the low-power laser irradiation, the mechanism of induction of this effect by the low-power lasers is not clear [43]. Our study is the first carried out to assess the telomere length in cardiac tissue in healthy animals after a low-power infrared laser irradiation. Notably, mRNA levels of TRF1 gene were altered in the cardiac tissue after the laser irradiation at 20 J cm^{-2} but not at 10 J cm^{-2} (Fig. 4a). Such a result suggests that the laser irradiation at 10 J cm^{-2} could induce telomere shortening and that the laser irradiation at 20 J cm^{-2} could increase the mRNA relative levels from TRF1 to maintain the telomere length in this group. These results further show that a careful analysis on the used protocols is required because, depending on the physical parameters and conditions of the irradiated tissue, the effects of low-power lasers can be adverse [43].

The laser-induced effects on the telomere length were also observed in the cardiac tissue of animals affected by the LPS-induced ALI. The low-power infrared laser irradiation at 10 J cm^{-2} increased the telomere length in heart tissue of rats after the LPS-induced ALI (Fig. 3b). However, no change in the relative mRNA levels of TRF1 and TRF2 were observed in the cardiac tissue of these animals upon the laser irradiation (Fig. 4b). The increase in telomere length observed in our results could have occurred because of the action of other proteins in the Sheltering complex, which also participates in the maintenance of the telomere length that could have been stimulated by the laser irradiation at 10 J cm^{-2} in cardiac cells of animals affected by LPS-induced sepsis. TRF1 and TRF2 are important proteins of the Shelterin complex, which bind to double-stranded telomere DNA and regulate the telomere length [44]. However, there are other proteins in this complex, such as the subcomplex POT1-TPP1, which is crucial to the telomere capping and telomere length regulation [35, 45]. In addition, all three TIN2 protein isoforms form a complex with TPP1/POT1 to stimulate the telomerase processivity and maintain the telomere integrity [46]. Also, RAP1 is one of the Shelterin complex components, which protects telomeres, but its role in such complex is not yet clear [47].

The data of this study showed telomere shortening and reduction in mRNA relative levels of TRF1 mRNA in cardiac tissue of animals in an experimental model of sepsis. Although the low-power infrared laser did not modulate the relative mRNA levels of TRF1 and TRF2 genes, the telomere length was increased at 10 J cm^{-2}, which indicates that, under adequate conditions of exposure, the low-power infrared laser could modulate the telomere maintenance in cardiac tissue in animals affected by LPS-induced ALI.

The beneficial effects of low-level laser therapy on the ARDS in animal models have been demonstrated [30, 48, 49]. Our results must be confirmed for humans. Although studies based on LPS-induced ALI in rats and mice have been carried out and important results have been reported [48, 50, 51], there are merits and drawbacks in such experimental models [27]. These should be considered as a limitation of our study when the effects of exposure to a low-power infrared laser on telomeres in heart tissue were extrapolated to humans. However, despite these limitations, our study suggests that the exposure to low-power lasers alters the telomere length, which could be considered for the development of clinical protocols based on laser-induced modulation of telomeres.

5 Conclusion

Our data show that, despite the telomere shortening in nontreated controls and mRNA levels of the TRF1 gene, the low-power infrared laser irradiation at 10 J cm^{-2} increased the telomere length in cardiac tissue of animals affected by LPS-induced ALI, which suggests that telomere maintenance is a part of the photobiomodulation effect induced by infrared radiation.

Author contributions All authors were responsible for the design and conduct of the research, analyzed and interpreted the data, performed the experimental protocols and the development of the project. All authors reviewed the manuscript before submission. All authors read and approved the final manuscript.

Availability of data and materials All data generated and analyzed during the study are included in the published article. The data are available upon request from the corresponding author.

Declarations

Conflict of interest The authors declare that they have no conflicts of interest.

References

1. But, Y., Kurdowska, A., & Allen, T. C. (2016). Acute lung injury: A clinical and molecular review. *Archives of Pathology and Laboratory Medicine, 140*, 345–350
2. Sadikot, R. T., Kolanjiyil, A. V., Kleinstreuer, C., & Rubinstein, I. (2017). Nanomedicine for treatment of acute lung injury and acute respiratory distress syndrome. *Biomed Hub., 2*, 1–12
3. Hariri, L., & Hardin, C. C. (2020). Covid-19, Angiogenesis, and ARDS Endotypes. *New England Journal of Medicine, 383*, 182–183
4. Goh, K. J., Choong, M. C., Cheong, E. H., Kalimuddin, S., Duu Wen, S., Phua, G. C., Chan, K. S., & HajaMohideen, S. (2020). Rapid progression to acute respiratory distress syndrome: Review of Current Understanding of Critical Illness from COVID-19 Infection. *Annals Academy Medicine Singapore, 49*, 108–118
5. Batah, S. S., & Fabro, A. T. (2021). Pulmonary pathology of ARDS in COVID-19: A pathological review for clinicians. *Respir Medicine, 176*, 106239
6. Mokra, D., & Kosutova, P. (2015). Biomarkers in acute lung injury. *Respiratory Physiology & Neurobiology, 209*, 52–58
7. Rungsung, S., Singh, T. U., Rabha, D. J., Kumar, T., CholenahalliLingaraju, M., Parida, S., Paulb, A., Sahoo, M., & Kumar, D. (2018). Luteolin attenuates acute lung injury in experimental mouse model of sepsis. *Cytokine, 110*, 333–343
8. Prescott, H. C., & Angus, D. C. (2018). Enhancing recovery from sepsis: A review. *JAMA, 319*, 62–75. https://doi.org/10.1001/jama.2017.17687
9. Ziesmann, M. T., & Marshall, J. C. (2018). Multiple organ dysfunction: The defining syndrome of sepsis. *Surgical Infections, 19*, 184–190
10. Sun, Y., Yao, X., Zhang, Q. J., Zhu, M., Liu, Z. P., Ci, B., Yang, X., Carlson, D., Rothermel, B. A., Sun, Y., Levine, B., Hill, J. A., Wolf, S. E., Minei, J. P., & Zang, Q. S. (2018). Beclin-1-dependent autophagy protects the heart during sepsis. *Circulation, 138*, 2247–2262
11. Drosatos, K., Lymperopoulos, A., Kennel, P. J., Pollak, N., Schulze, P. C., & Goldberg, I. J. (2014). Pathophysiology of sepsis-related cardiac dysfunction: Driven by inflammation, energy mismanagement, or both? *Current Heart Failure Represent, 12*, 130–140
12. Zaky, A., Deem, S., Bendjelid, K., & Treggiari, M. M. (2014). Characterization of cardiac dysfunction in sepsis: An ongoing challenge. *Shock, 41*, 12–24
13. Weischer, M., Bojesen, S. E., Cawthon, R. M., Freiberg, J. J., Tybjaerg-Hansen, A., & Nordestgaard, B. G. (2011). Short telomere length, myocardial infarction, ischemic heart disease, and early death. *Arterioscler Thromb Vascular Biology, 32*, 822–829
14 Brouilette, S. (2003). White cell telomere length and risk of premature myocardial infarction. *Arterioscler Thromb Vascular Biology, 23*, 842–846
15. Terai, M., Izumiyama-Shimomura, N., Aida, J., Ishikawa, N., Sawabe, M., Arai, T., Fujiwara, M., Ishii, A., Nakamura, K., & Takubo, K. (2013). Association of telomere shortening in myocardium with heart weight gain and cause of death. *Science and Reports, 3*, 2401
16. Sharifi-Sanjani, M., Oyster, N. M., Tichy, E. D., Bedi, K. C., Harel, O., Margulies, K. B., & Mourkioti, F. (2017). Cardiomyocyte-specific telomere shortening is a distinct signature of heart failure in humans. *Journal of American Heart Association, 6*, e005086
17. Martínez, P., & Blasco, M. A. (2018). Heart-breaking telomeres. *Circulation Research, 123*, 787–802
18. Sanders, J. L., & Newman, A. B. (2013). Telomere length in epidemiology: A biomarker of aging, age-related disease, both, or neither? *Epidemiology Version, 35*, 112–131
19 Turner, K. J., Vasu, V., & Griffin, D. K. (2019). Telomere biology and human phenotype. *Cells, 8*, E73
20. Booth, S. A., & Charchar, F. J. (2017). Cardiac telomere length in heart development, function, and disease. *Physiological Genomics, 49*, 368–384
21 Anderson, R., et al. (2019). Length-independent telomere damage drives post-mitotic cardiomyocyte senescence. *EMBO Journal, 38*, e100492
22. Erdel, F., Kratz, K., Willcox, S., Griffith, J. D., Greene, E. C., & de Lange, T. (2017). Telomere recognition and assembly mechanism of mammalian Shelterin. *Cell Reports, 18*, 41–53
23 Da Silva NetoTrajano, L. A., Stumbo, A. C., da Silva, C. L., Mencalha, A. L., & Fonseca, A. (2016). Low-level infrared laser modulates muscle repair and chromosome stabilization genes in myoblasts. *Lasers Medical Science, 31*, 1161–1167
24. Da Silva NetoTrajano, L. A., Trajano, E. T. L., da Silva Sergio, L. P., Teixeira, A. F., Mencalha, A. L., Stumbo, A. C., & de Souza da Fonseca, A. (2018). Photobiomodulation effects on mRNA levels from genomic and chromosome stabilization genes in injured muscle. *Lasers Medical Science, 33*, 1513–1519
25. De Souza-da-Fonseca, A., Mencalha, A. L., Araújo-de-Campos, V. M., Ferreira-Machado, S. C., de Freitas-Peregrino, A. A., Geller, M., & de Paoli, F. (2013). DNA repair gene expression in biological tissues exposed to low-intensity infrared laser. *Lasers in Medical Science, 28*, 1077–1084
26. Trajano, E. T. L., Mencalha, A. L., Monte-Alto-Costa, A., Pôrto, L. C., de Souza, A., & da Fonseca, . (2014). Expression of DNA repair genes in burned skin exposed to low-level red laser. *Lasers in Medical Science, 29*, 1953–1957
27. Trajano, L. A. S. N., Sergio, L. P. S., Silva, C. L., Carvalho, L., Mencalha, A. L., Stumbo, A. C., & Fonseca, A. S. (2016). Low-level laser irradiation alters mRNA expression from genes involved in DNA repair and genomic stabilization in myoblasts. *Laser Physics Letter, 13*, 075601
28. Chen, H., Bai, C., & Wang, X. (2010). The value of the lipopolysaccharide-induced acute lung injury model in respiratory medicine. *Expert Review of Respiratory Medicine, 4*, 773–783
29. Fodor, R. S., Georgescu, A. M., Cioc, A. D., Grigorescu, B. L., Cotoi, O. S., Fodor, P., Copotoiu, S. M., & Azamfirei, L. (2015). Time- and dose-dependent severity of lung injury in a rat model of sepsis. *Romanian Journal of Morphology and Embryology, 56*, 1329–1337
30. Brown, D. L. (2017). Practical stereology applications for the pathologist. *Veterinary Pathology, 54*, 358–368
31. Sergio, L. P. S., Trajano, L. A. S. N., Thomé, A. M. C., Mencalha, A. L., de Paoli, F., & da Fonseca, A. S. (2018). Low power infrared laser modifies the morphology of lung affected with acute injury induced by sepsis. *Laser Physics, 28*, 065601
32. Jiang, Y. X., Dai, Z. L., Zhang, X. P., Zhao, W., Huang, Q., & Gao, L. K. (2015). Dexmedetomidine alleviates pulmonary edema by upregulating AQP1 and AQP5 expression in rats with acute lung injury induced by lipopolysaccharide. *Journal of Huazhong University Science and Technology, 35*, 684–688
33. Cawthon, R. M. (2002). Telomere measurement by quantitative PCR. *Nucleic Acids Research, 30*, 47e
34. Livak, K. J., & Schmittgen, T. D. (2001). Analysis of relative gene expression data using real-time quantitative PCR and the 2 (-Delta Delta C(T)) Method. *Methods, 25*, 402–408
35. Ludlow, A. T., Gratidão, L., Ludlow, L. W., Spangenburg, E. E., & Roth, S. M. (2017). Acute exercise activates p38 mapk and increases the expression of telomere-protective genes in cardiac muscle. *Experiment of Physiology, 102*, 397–410

36. de Lange, T. (2010). How shelterin solves the telomere end-protection problem. *Cold Spring Harbor Symposia on Quantitative Biology., 75*, 167–177
37. Haycock, P. C., Heydon, E. E., Kaptoge, S., Butterworth, A. S., Thompson, A., & Willeit, P. (2014). Leucocyte telomere length and risk of cardiovascular disease: systematic review and meta-analysis. *BMJ, 349*, g4227–g4227
38. Oliveira, N. M., et al. (2016). Sepsis induces telomere shortening: A potential mechanism responsible for delayed pathophysiological events in sepsis survivors? *Molecular Medicine, 22*, 886–891
39. Liu, S., et al. (2019). Peripheral blood leukocyte telomere length is associated with survival of sepsis patients. *European Respiratory Journal, 55*, 1901044
40 Scheller-Madrid, A., Rode, L., Nordestgaard, B. G., & Bojesen, S. E. (2016). Short telomere length and ischemic heart disease: Observational and genetic studies in 290 022 individuals. *Clinical Chemistry, 62*, 1140–1149
41. Fonseca, A. S., Magalhães, L. A. G., Mencalha, A. L., Ferreira-Machado, S. C., Geller, M., & Paoli, F. (2014). Low-intensity red and infrared lasers on XPA and XPC gene expression. *Laser Physics Letter, 11*, 095601
42. Biasibetti, M., Rojas, D. B., Hentschke, V. S., Moura, D. J., Karsten, M., Wannmacher, C. M. D., Saffi, J., & Dal Lago, P. (2014). The influence of low-level laser therapy on parameters of oxidative stress and DNA damage on muscle and plasma in rats with heart failure. *Lasers in Medical Science, 29*, 1895–1906
43. Sergio, L. P. S., Silva, A. P. A., Amorim, P. F., Campos, V. M. A., Magalhães, L. A. G., Paoli, F., & Fonseca, A. S. (2015). DNA damage in blood cells exposed to low-level lasers. *Lasers in Medical Science, 47*, 361–368
44. Fonseca, A. S., Presta, G. A., Geller, M., & Paoli, F. (2011). Low intensity infrared laser induces filamentation in *Escherichia coli* cells. *Laser Physics, 21*, 1829–1837
45. Rice, C., Shastrula, P. K., Kossenkov, A. V., Hills, R., Baird, D. M., Showe, L. C., Doukov, T., Janicki, S., & Skordalakes, E. (2017). Structural and functional analysis of the human POT1-TPP1 telomeric complex. *Nature Communications, 8*, 14928
46. Aramburu, T., Plucinsky, S., & Skordalakes, E. (2020). POT1-TPP1 telomere length regulation and disease. *Computational and Structural Biotechnology Journal, 18*, 1939–1946
47. Pike, A. M., Strong, M. A., Ouyang, J. P. T., & Greider, C. W. (2019). TIN2 Functions with TPP1/POT1 To Stimulate Telomerase Processivity. *Molecular and Cellular Biology, 39*, e00593-e618
48. Martínez, P., Gómez-López, G., Pisano, D. G., Flores, J. M., & Blasco, M. A. (2016). A genetic interaction between RAP1 and telomerase reveals an unanticipated role for RAP1 in telomere maintenance. *Aging Cell, 15*, 1113–1125
49. Oliveira, M. C., Jr., Greiffo, F. R., Rigonato-Oliveira, N. C., Custódio, R. W., Silva, V. R., Damaceno-Rodrigues, N. R., Almeida, F. M., Albertini, R., Lopes-Martins, R. A., de Oliveira, L. V., de Carvalho, P. T., Ligeiro-de-Oliveira, A. P., Leal, E. C., Jr., & Vieira, R. P. (2014). Low level laser therapy reduces acute lung inflammation in a model of pulmonary and extrapulmonary LPS-induced ARDS. *Journal of Photochemistry Photobiology B, 134*, 57–63
50. Sergio, L. P. S., Thomé, A. M. C., Trajano, L. A. S. N., Mencalha, A. L., da Fonseca, A. S., & de Paoli, F. (2018). Photobiomodulation prevents DNA fragmentation of alveolar epithelial cells and alters the mRNA levels of caspase 3 and Bcl-2 genes in acute lung injury. *Photochemical & Photobiological Sciences, 17*, 975–983
51. Fazza, T. F., Pinheiro, B. V., da Fonseca, L. M. C., Sergio, L. P. D. S., Botelho, M. P., Lopes, G. M., de Paoli, F., da Fonseca, A. S., Lucinda, L. M. F., & Reboredo, M. M. (2020). Effect of low-level laser therapy on the inflammatory response in an experimental model of ventilator-induced lung injury. *Photochemical & Photobiological Sciences, 19*, 1356–1363
52. Kashanskaia, E. P., & Fedorov, A. A. (2009). Low-intensity laser radiation in the combined treatment of patients with chronic obstructive bronchitis. *Voprosy Kurortologii, Fizioterapii i Lechebnoi Fizicheskoi Kultury, 2*, 19–22